ELSEVIER

Cement and Concrete Composites **20** (1998) 365–375
0958-9465/98/$ — see front matter

PII:S0958-9465(98)00017-1

Flexural Properties of Steel Fiber-reinforced Concretes at Low Temperatures

M. Pigeon* & R. Cantin

Centre de recherche interuniversitaire sur le béton (Sherbrooke-Laval), Université Laval, Sainte-Foy, Québec, Canada G1K 7P4

Abstract

The mechanical properties of steel fiber-reinforced concrete (SFRC) at low temperatures were determined using the standard ASTM C1018 flexure test. The tests were performed at normal room temperature (20°C) at −10°C and at −30°C. In addition to the temperature, the variables investigated were the type of cement (both normal Portland cement and silica fume cement were used), the water/binder ratio (0.45, 0.35 and 0.30), the type of fiber (two very different geometries were chosen) and the fiber dosage (40 kg/m^3 and 60 kg/m^3). The results show that the toughness of SFRC under flexural loading increases with a decrease in temperature. This increase appears to be related to the increase in the strength of the matrix at low temperatures (because of the freezing of water in the capillary pores), which increases the energy required for fiber pull-out. The toughness increase was observed both for normal and high performance concretes, and for both types of fibers at both dosages. In these tests, the influence of the fiber geometry was found to be relatively small. © *1998 Elsevier Science Ltd. All rights reserved*

Keywords: silica fume, temperature, flexural.

INTRODUCTION

The mechanical properties of steel fiber-reinforced concrete (SFRC) have been the subject of numerous studies during the last 20 years and are now fairly well known.[1] These investigations, however, have generally been performed at room temperature (20°C). But at low temperatures, particularly below freezing point, the mechanisms that control the properties of SFRC could be quite different, since the mechanical properties of both steel and concrete vary quite significantly with temperature.

Like most solid materials, steel and concrete contract when the temperature decreases. This is because of the reduction of the kinetic energy of the atoms, which induces a reduction of the thermal agitation. Because of the asymmetry of the curve representing the potential energy versus the inter atomic distance for a given material, the average equilibrium distance between atoms is reduced, and this reduction continues until the temperature reaches −273°C at which point there is no agitation left.[2] This decrease of the distance between the atoms causes an increase in strength because the attractive forces between the atoms increase. The brittleness of the bond also increases with the attractive forces. Steel and concrete are thus both more resistant, but also more brittle, at low temperatures.

In concrete, in addition to the reduction of the distance between the atoms, low temperatures have another significant effect. As the temperature decreases below 0°C, water in the pores begins to freeze. This causes an increase in strength since capillary pores become filled with a solid material that has a significant load bearing capacity and that develops strong bonds with the hardened cementitious matrix. It is further probable that the frozen water increases the fracture toughness, and prevents stress corrosion, which also increases strength.[3] The

*To whom correspondence should be addressed.

increase in strength at low temperatures would thus depend for the most part on the freezable water content. This has been noticed by Miura[4] who observed that the increase in strength at low temperatures varies almost linearly with the water content of the mixture.

Stavena *et al.*[5] tested 0.5 water/cement ratio concretes made with two different steel fibers at two different dosages under flexure at low temperatures. The test results indicate that both strength and toughness increase as the temperature decreases. Strength and toughness at low temperatures were also found to increase with the fiber dosage.

RESEARCH OBJECTIVES

This investigation is part of a research project aimed at the development of SFRC mixtures adapted to the Canadian climate, i.e. that are durable and that have good mechanical properties at low temperatures. This paper describes the part of the project related to the mechanical behavior of SFRC at low temperatures. Only limited data concerning this aspect of the performance of SFRC are available at the present time,[5] and the tests described were thus performed to generate additional data concerning the properties of SFRC at low temperatures.

TEST PARAMETERS

The variables selected for this investigation are the following: the water/binder ratio, the type of fibers, the fiber dosage, the type of cement and, of course, the temperature (see Table 1 for the detailed list of variables). The maximum water/binder ratio corresponds to the upper limit in Canada for concrete exposed to de-icer salt applications, and the minimum to the practical lower limit when macro steel fibers are used.

Table 1. List of variables

Variable	*Values*
Water/binder ratio	0.45, 0.35, 0.30
Binder	Canadian type 10 (OPC) Silica fume blended cement (8.5% SF)
Fiber type	Crimped End-deformed
Fiber dosage	40 kg/m^3 and 60 kg/m^3
Test temperature	20°C, −10°C and −30°C

Both normal Portland cement and silica fume cement were used since these are the two most commonly used binders in SFRC. The characteristics of the two (macro) steel fibers selected for the tests are shown in Table 2. They represent the two most typical shapes for such fibers: one deformed along its length (A), and the other with an anchorage at both ends (B). The 40 kg/m^3 dosage is generally considered as an average dosage that significantly improves the toughness of concrete, and 60 kg/m^3 is a practical (economical) upper limit to macro steel fiber dosage. The three temperatures selected for the tests (20°C, −10°C and −30°C) represent, respectively, a normal (reference) temperature, a normal or average winter temperature, and a very low temperature such as occurs in Canada during the winter.

EXPERIMENTAL

Equipment and test procedures

A special cell using liquid nitrogen as a cooling agent was used for this investigation (Fig. 1). This cell, developed at Laval University in a previous project,[6] can be placed in the loading frame and has a temperature control system. The temperature inside the concrete specimens is monitored with thermocouples. Preliminary tests showed that there was only a small difference (1 or 2°C) between the temperature in the middle of the specimen and close to the surface. Because of this, it was decided to use a single thermocouple per specimen.

To reduce the thermal shock as well as the time required for each test and the liquid nitrogen consumption, each specimen for the −30°C tests was precooled in a −18°C freezer for approximately 16 h. After this period, the specimen was placed immediately in the test chamber that had been precooled to −50°C to accelerate the temperature decrease inside the specimen. The temperature of the chamber was set at −30°C only when the specimen had reached a temperature close to this value. The tests at −10°C were performed also on specimens precooled at −18°C, but only after the temperature inside the specimens had been increased to (and stabilized at) −10°C.

The (flexure) tests were performed on standard specimens (100 mm × 100 mm × 350 mm prisms resting on two supports placed

Table 2. Fiber characteristics

Fiber	*Geometry*	*Cross-sectional shape*	*Length (mm)*	*Diameter (mm)*	*Weight (g)*	*No./kg*
Deformed	crimped (A)	circular	60	1.0	0.420	2380
With conical anchorages	end-deformed (B)	circular	54	1.0	0.403	2480

300 mm apart) at a vertical displacement rate of 0.1 mm/min. A mobile frame and a potentiometer capable of measuring displacements at temperatures as low as −70°C were used to determine the displacement at the neutral axis.

All specimens were cured in lime-saturated water for 28 days and tested immediately after this period, i.e. they were not allowed to dry before being frozen.

In addition to the ASTM C1018 flexure tests (four specimens were used for each test condition, i.e. type of concrete and temperature of test), compressive strength tests (ASTM C39) and air void characteristic determinations (ASTM C457) were performed.

Materials and mixture composition

The same normal Portland cement and the same silica fume blended cement (containing 8.5% by mass of silica fume) were used throughout. The coarse aggregate was a crushed granitic gneiss with a particle size that ranged between 14 mm and 5 mm for the 0.45 and the 0.35 water/binder ratio mixtures, and a particle size between 10 mm and 2.5 mm for the 0.30 water/binder ratio mixtures. A granitic sand with a fineness modulus varying between 2.3 and 2.6 was used for all mixtures. The superplasticizer was a naphthalene-based admixture, the water reducer was an hydroxycarboxylic acid, and the air-entraining admixture was made of salts of fatty acids.

In order to reduce the number of tests, it was decided for this series of experiments to use the so-called *plan d'expériences* method to determine the characteristics of the mixtures to be prepared and the temperature at which they would be tested. Considering the temperature and the water/binder ratio as the two main numerical variables, the test program was divided into six series of tests, each series forming a 'square' such as presented in Fig. 2, each corner of the 'square' representing a combination of the 'extreme' values of these two parameters (0.45 and 0.30 for the water/binder ratio, and 20°C and −30°C for the temperature), and the middle point corresponding to the intermediate values (0.35 and −10°C). Fig. 2 describes the six 'squares' that were selected, each corresponding to a given cement, fiber and fiber dosage. The combination of the type 10 cement with the highest dosage of fiber was not included in the test program.

The compositions of the 18 (air-entrained) mixtures that were prepared are presented in Table 3, together with the fresh concrete properties, the compressive strength at 28 days and the air void content determined on the hardened concrete. In this table, each group of

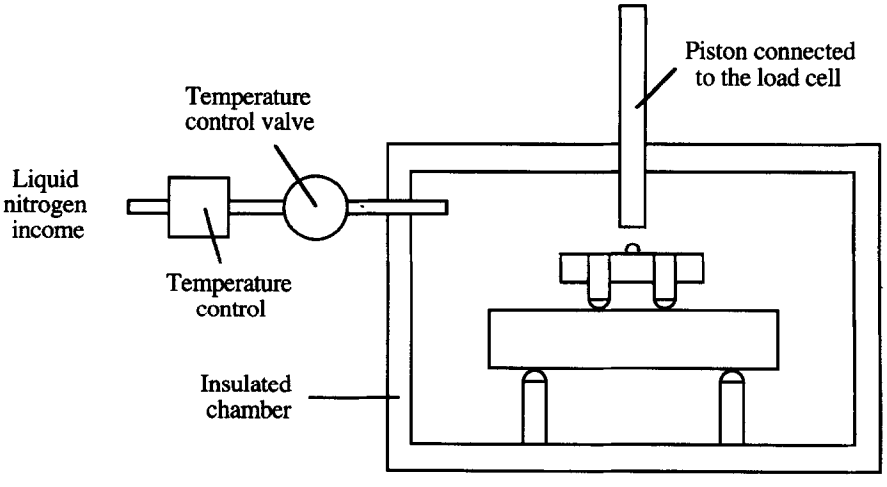

Fig. 1. View of the apparatus used for the low temperature tests.

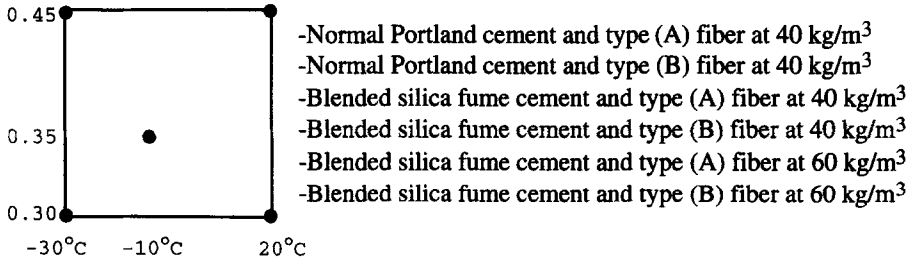

Fig. 2. Typical test 'square' and description of the variables for each of the 'squares'.

three mixtures corresponds to a test 'square'. The mixture compositions given are the actual values that were obtained. It can be seen in this Table that the air content is variable since it is very difficult to control air-entrainment, especially in fiber-reinforced concrete. This explains in good part, the variability of the compressive strength for a given mixture (i.e. with a given water/binder ratio, binder and fiber dosage).

RESULTS AND DISCUSSION OF THE FLEXURE TESTS

A total of 120 specimens were tested in flexure during this investigation. The results of these tests are summarized in Figs 3 and 4. Figure 3 gives, for each test condition (i.e. type of concrete and temperature of test), the average value of the peak load for the four specimens. Fig. 4 gives, for each test condition, the average value (for the four specimens) of the area under the load-displacement curve up to a deflection of 1 mm. In each of these two figures, there are six group of results that correspond to the six basic series of tests as defined in the previous section.

To illustrate the variability of this type of test, and also partly explain why the area under the load-displacement curve (the deformation energy) up to a deflection of 1 mm was selected as the main analysis criterion, the four individual load-displacement curves for six of the 30 different test conditions are presented in Figs 5–10. Figs 5–7 show some of the results obtained with fiber A, and Figs 8–10 some of the results obtained with fiber B.

The variability of the test results in Figs 5–10 is mainly caused by the variability of the number of fibers found at the main flexure crack. It is extremely important to consider this variability when analyzing the average results presented in Figs 3 and 4. In Fig. 4, for instance, it can be seen that, with the silica fume cement at a water/binder ratio of 0.45, the

Table 3. Mixture characteristics

Mixture	*W/B ratio*	*Fiber type*	*Cement type*	*Mixture composition (kg/m³)*					*Admixture dosages (ml/m³)*			*Slump (mm)*	*Air content (%)*		*Spacing factor (μm)*	*Comp. strength (MPa)*
				Cement	*Water*	*Sand*	*Stone*	*Fiber*	*W.R.*	*A.E.A.*	*S.P.*		*Fresh*	*Hardened*		
1	0.45	A	T10	375	167	805	982	40.2	750	91	476	75	5.4	3.8	167	40.1
2	0.29	A	T10	431	123	882	893	38.7	0	1290	11447	50	7.2	5.9	238	50.6
3	0.34	A	T10	439	151	818	998	40.9	0	435	4376	90	3.8	2.7	343	49.4
4	0.45	A	SF	362	162	775	946	38.8	723	79	547	125	8.5	6.8	132	48.0
5	0.30	A	SF	416	123	856	855	37.5	0	836	6312	160	11.0	5.5	232	66.5
6	0.35	A	SF	431	151	803	980	40.2	0	474	4741	90	5.0	4.1	255	66.7
7	0.45	B	T10	366	164	785	957	39.2	733	93	755	100	7.6	6.5	134	38.2
8	0.30	B	T10	424	127	872	872	38.5	0	1277	11194	80	9.0	6.9	150	46.5
9	0.35	B	T10	419	145	781	952	39.0	0	725	4702	120	8.0	6.3	135	42.3
10	0.43	B	SF	369	158	793	967	39.7	746	84	564	90	6.8	6.9	128	50.0
11	0.29	B	SF	417	123	858	860	37.5	0	837	6275	100	10.0	9.2	111	56.0
12	0.35	B	SF	413	144	771	939	38.6	0	526	4093	95	8.5	7.9	88	48.6
13	0.45	A	SF	362	162	776	946	58.1	722	81	634	145	8.0	7.6	165	49.2
14	0.30	A	SF	452	134	845	846	58.0	0	914	5977	210	8.5	7.3	278	63.7
15	0.35	A	SF	417	149	743	902	56.8	0	421	4594	190	10.0	9.2	141	51.1
16	0.45	B	SF	355	159	761	928	57.0	711	87	711	155	9.5	8.2	107	46.3
17	0.30	B	SF	443	131	885	885	59.0	0	882	6656	100	6.2	6.0	379	69.6
18	0.36	B	SF	408	145	741	903	56.3	0	413	4500	210	11.0	8.9	116	50.9

total deformation energy (at −30°C) is lower for fiber A than for fiber B, at the same 40-kg/m^3 dosage. However, considering the individual results in Figs 6 and 8, the significance of this difference could probably be questioned, since a change in only one of the four individual results could almost completely eliminate this difference.

Various ways have been suggested to quantify the benefits obtained under flexural loading with the use of macro steel fibers.[7,8] Considering the load-displacement curves shown in Figs 5–10, it is clear that no single value can fully describe the behavior of SFRC. If the value is based on the first crack displacement, any error in the determination of this displacement is reflected in the result obtained. It was thus considered more reliable to measure the area under the load-displacement curve (the deformation energy) up to a limiting value of the displacement (particularly considering that the formation of ice on the measuring device prevented, in certain cases, the correct measurement of the displacement before the peak load). Two values were selected: 1 mm and 2 mm. After having examined the results obtained with these two values, no very significant relative differences between the results for the various test conditions were observed, and it was decided to perform the analysis using only the energy value up to a displacement of 1 mm.

The results in Fig. 3 indicate clearly that, for each of the six group of results, the peak load increases as the temperature decreases. This increase is apparently related to the amount of freezable water in the matrix, since it is much higher at a water/binder ratio of 0.45 than at 0.30, and it is also much higher for the normal cement mixtures than for the silica fume mixtures. As previously mentioned, such an increase in strength is mainly caused by the formation of ice in the capillary pores, which increases the bearing capacity of the matrix and the resistance to crack propagation. Contrary to what was observed for the compressive strength test results (Table 3), the results in Fig. 3 indicate no large significant differences between the mixtures made with the normal cement and

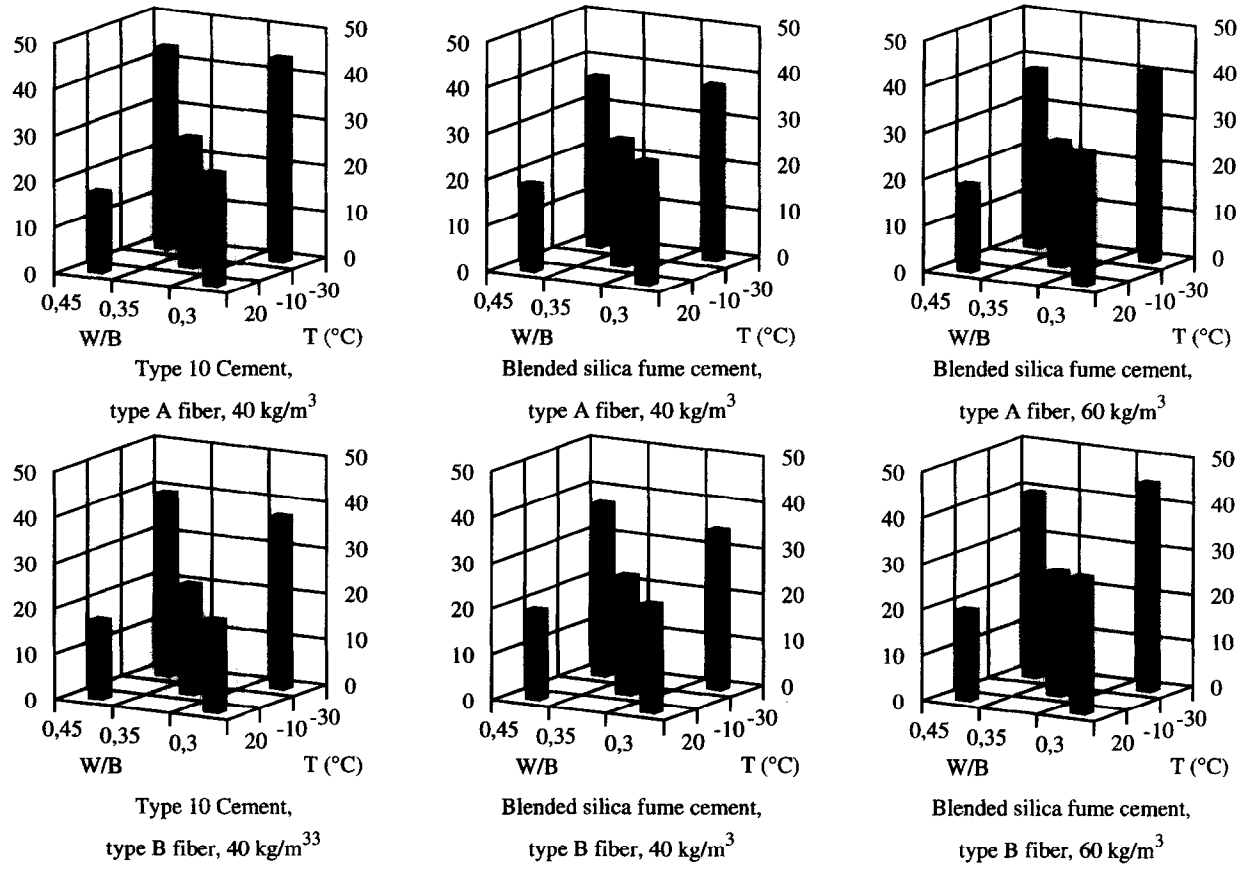

Fig. 3. The average value of the peak load for the four specimens for each test condition (i.e. type of concrete and temperature of test).

those made with the silica fume cement. It thus appears that the presence of silica fume had a larger influence on the compressive strength than on the flexural strength as determined from the peak load on the load versus displacement curves.

No major differences between the six groups of results can be observed in Fig. 3. As regards the peak load obtained under third point loading, the type of fiber as well as the dosage (in the range tested) thus apparently have little influence, which could be expected considering that steel fibers at volume fractions lower than the critical value have little influence on flexural strength. As could be expected, at 20°C, the peak load is always higher at a water/binder ratio of 0.30 than at 0.45. However, at −30°C, the results are quite similar. It should further be noted that some of the strength variations can be caused in part by air content variations in these air-entrained concretes.

Figure 4 shows that, for each of the six groups of concretes, the total deformation energy (the area under the load-displacement curve) up to a 1-mm deflection, similar to the peak load, increases as the temperature decreases. Although both concrete and steel are more brittle at low temperatures, SFRC is not, probably because the main energy absorption mechanism is the pull-out of the fibers from the matrix, and this mechanism can still exist at low temperatures. There is in fact generally an increase in deformation energy at low temperatures, which can globally be related to the increased strength of the matrix and thus to the increased energy requirement during the pull-out of the fibers. However, the increase in energy absorption is not always proportional to the increase in strength, indicating that, to a certain extent, the increased brittleness of the fibers can nevertheless have an influence on energy absorption. This increase in energy absorption is generally small at −10°C, but quite significant at −30°C, which confirms its relation with the strength of the matrix at low temperatures.

For the concretes made with fiber A, the increase in energy absorption at low temperatures is similar for water/binder ratio of 0.45 and 0.30 (Fig. 4), and it appears to be closely

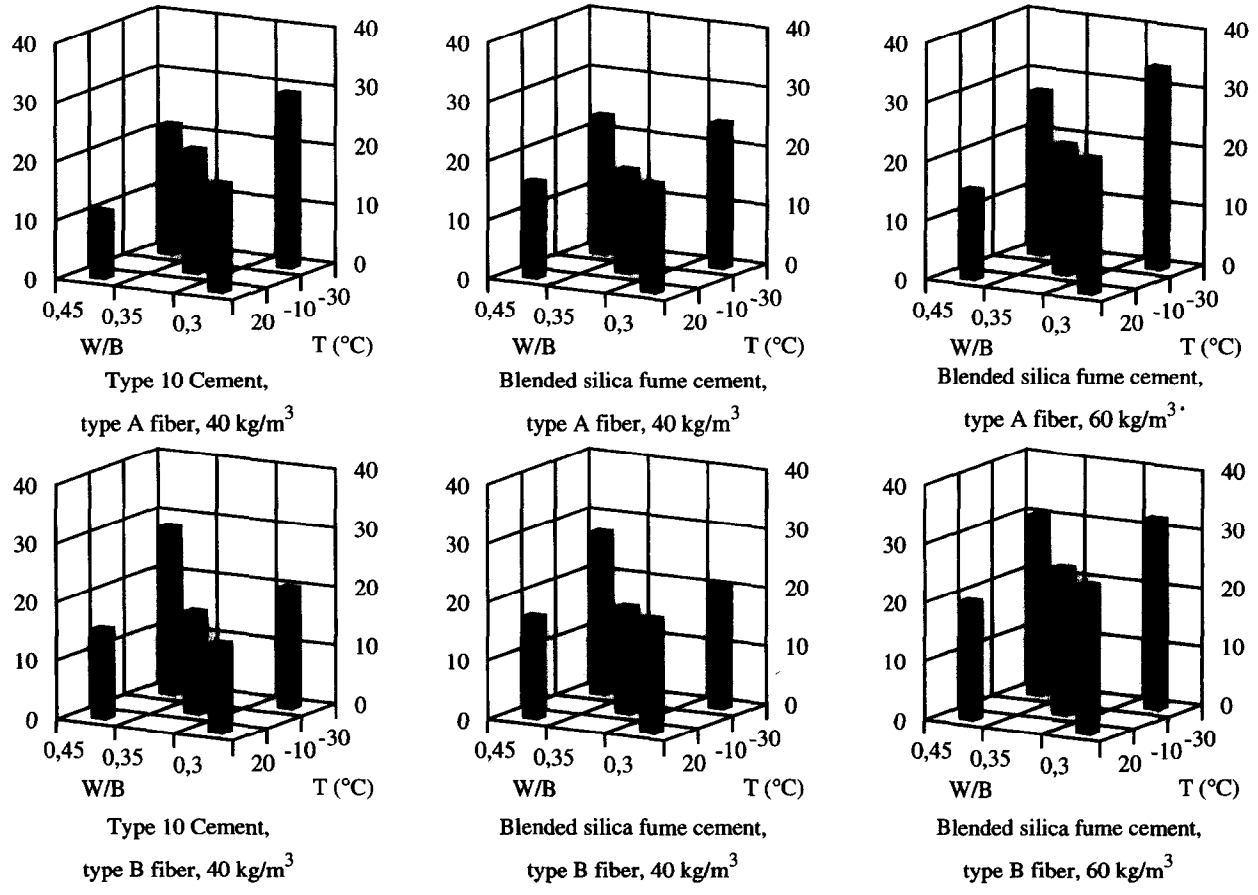

Fig. 4. Area under the load-displacement curve up to a deflection of 1 mm for each test condition.

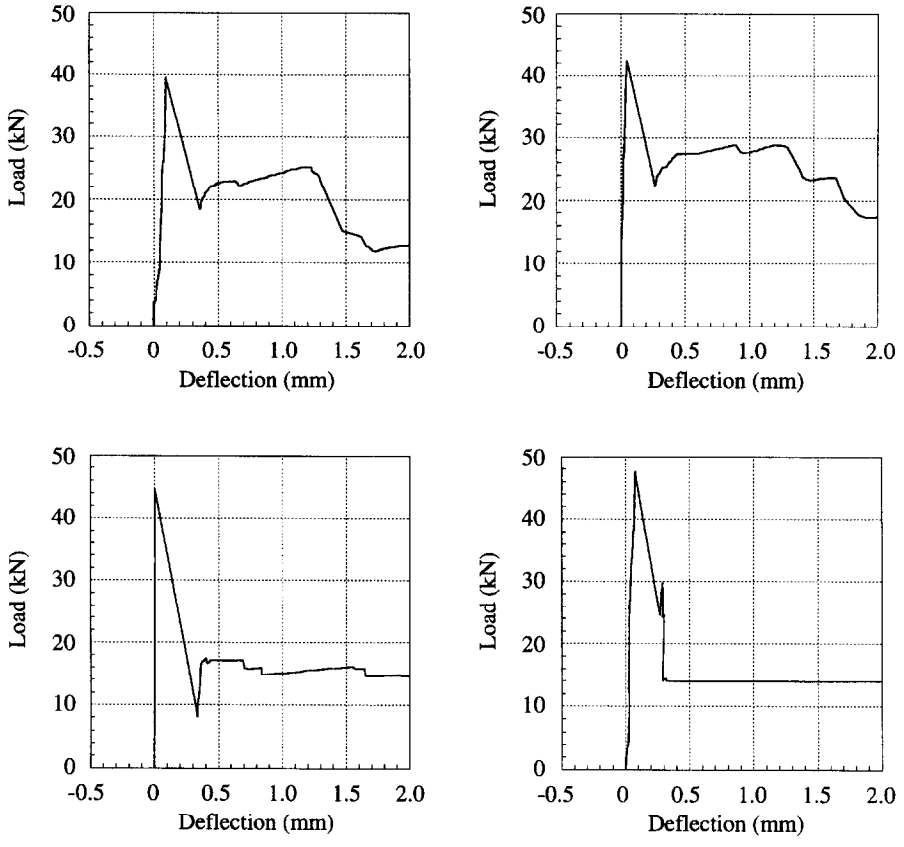

Fig. 5. Fiber A, 40 kg/m^3, type 10 cement, W/B = 0.45, −30°C.

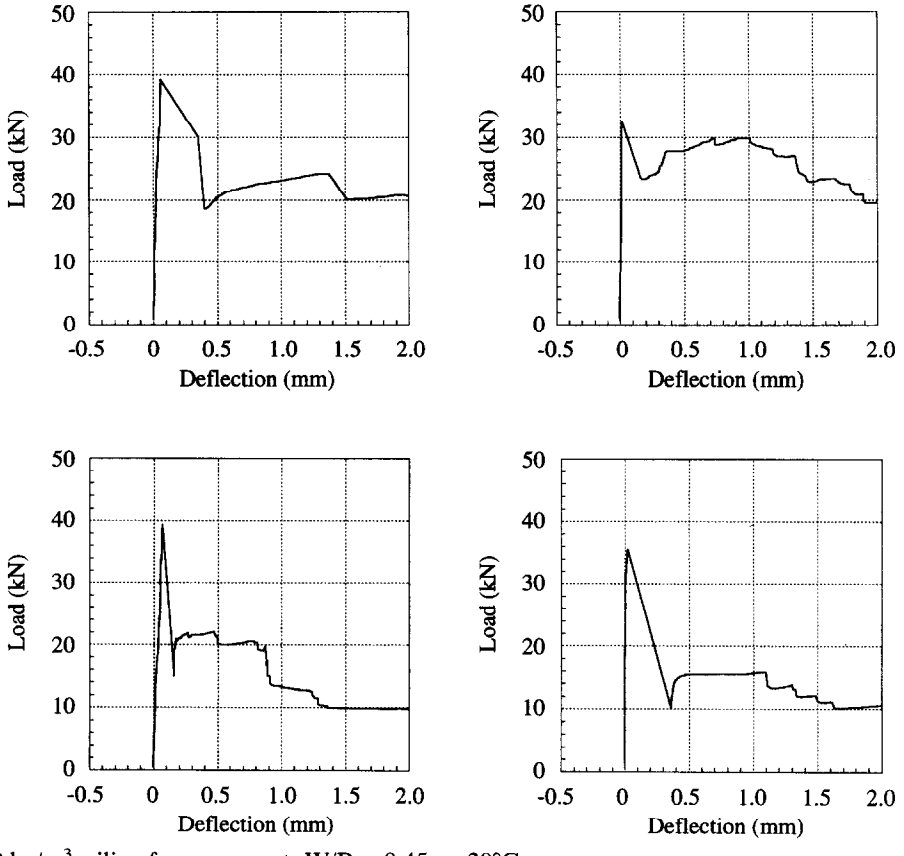

Fig. 6. Fiber A, 40 kg/m^3, silica fume cement, W/B = 0.45, −30°C.

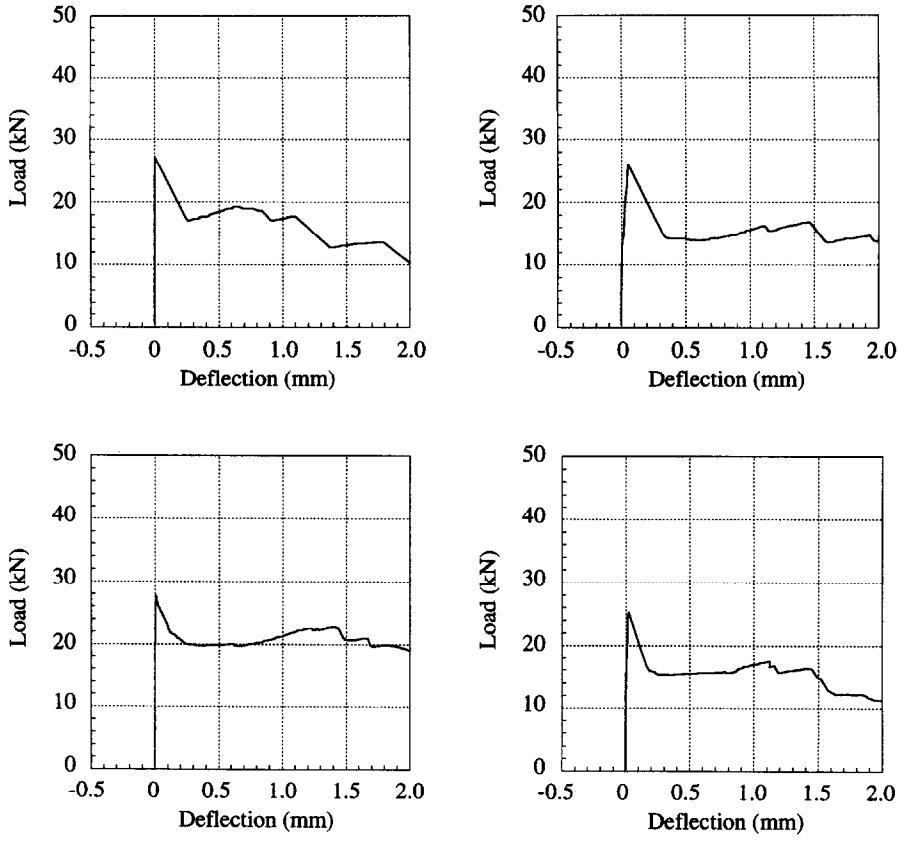

Fig. 7. Fiber A, 40 kg/m^3, silica fume cement, W/B = 0.30, 20°C.

linked with the increase in the peak load. For the concretes made with fiber B at a water/binder ratio of 0.30, however, the increase in energy is generally smaller than the increase in the peak load. Although it can be seen from Fig. 4 that the results for the six groups of mixtures are quite similar, the geometry of the fiber has also some influence on the behavior of SFRC under flexural loading at low temperatures. For reasons that are still not clear, it appears that, at a certain point, an increase in the strength of the matrix has a smaller effect for a fiber with 'positive' anchors at both ends. This could be explained by the pull-out mechanisms that are quite different for the two fibers investigated. It is possible that fiber B could be more susceptible to break in a stronger matrix, since it mainly relies on the bearing strength of the matrix around the anchor to resist pull-out, whereas the crimped fiber mainly relies on the interfacial bonding strength (which appears to increase significantly when water freezes).

From the values in Fig. 4, it is clear that the fiber dosage, in the range investigated, had a relatively small influence. The energy values measured at 60 kg/m^3 are generally higher than at 40 kg/m^3, but not by 50%. It can be hypothesized that the mechanisms of energy absorption by pull-out are quite similar at both dosages, but that a closer fiber spacing has a somewhat negative influence, probably by increasing the possibility of interaction between the matrix zones affected by each individual fiber. The values in Fig. 4 also show that the type of cement only had a modest influence, the energy absorbed being generally lower in the mixtures made with the type 10 cement, but mainly when tested at 20°C. At −30°C, the influence of the cement is reduced, since the water in the capillary pores is frozen and thus the pore size distribution has less influence.

The results obtained (see Fig. 3 and Fig. 4) tend to indicate that the relationship between water/binder ratio, temperature and energy under the load-displacement curve, as well as that between water/binder ratio, temperature and peak load, cannot be approximated with the model of the first degree (i.e. a planar surface can not accommodate the five points on the three-dimensional graph), but could be with

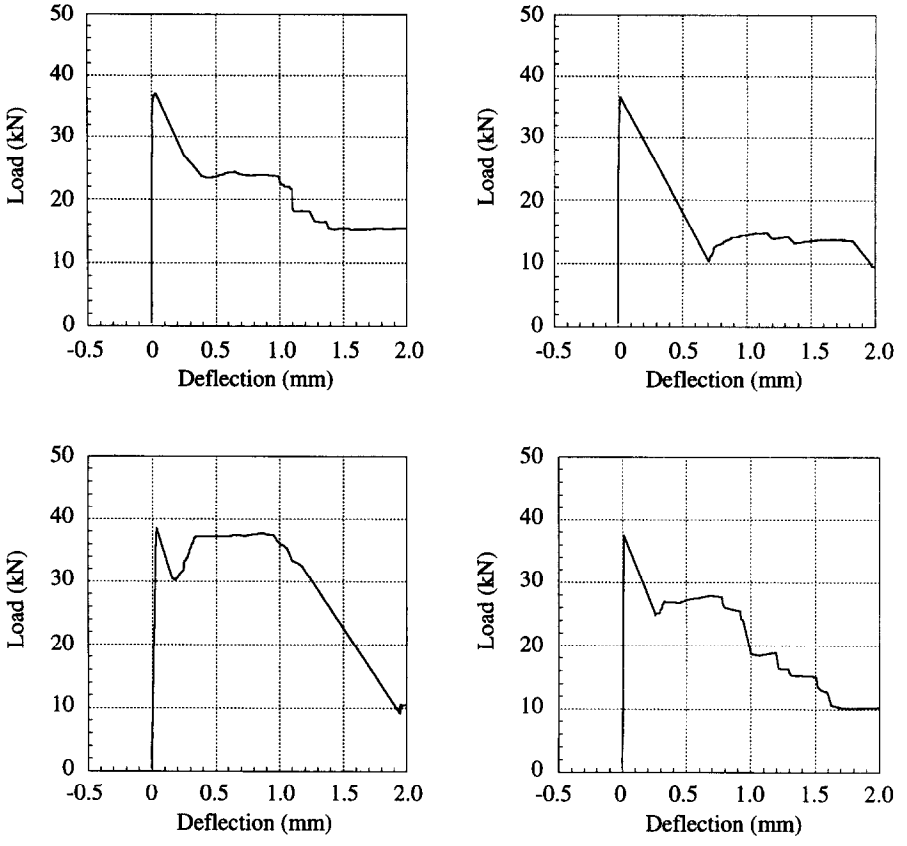

Fig. 8. Fiber B, 40 kg/m^3, silica fume cement, W/B = 0.45, −30°C.

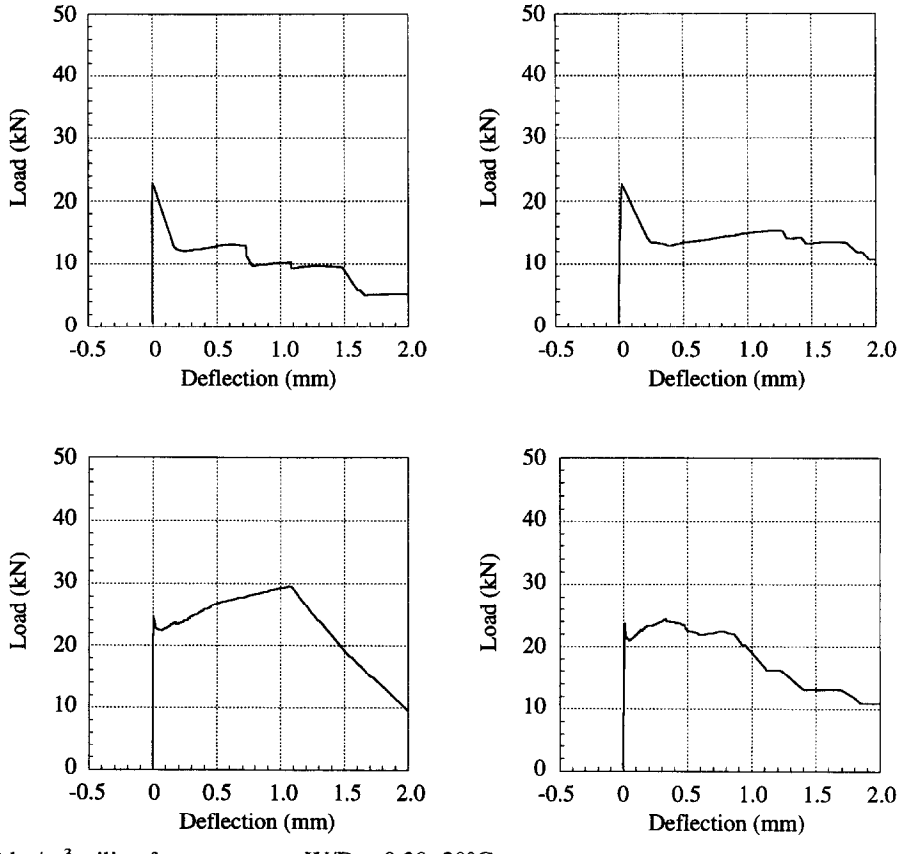

Fig. 9. Fiber B, 40 kg/m^3, silica fume cement, W/B = 0.30, 20°C.

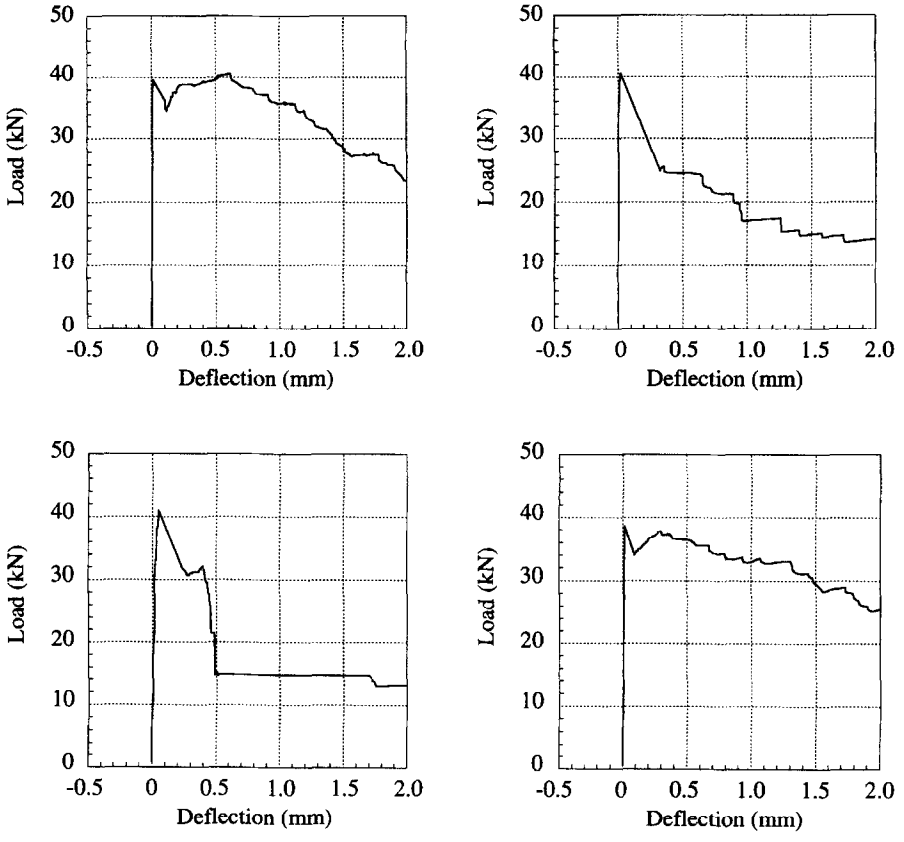

Fig. 10. Fiber B, 60 kg/m^3, silica fume cement, W/B = 0.45, −30°C.

a model of the second degree (a curved surface).

CONCLUSION

On the basis of the results presented in this paper, it can be concluded that the toughness of SFRC under flexural loading increases as the temperature decreases. This increase is small at −10°C, but generally quite significant at −30°C. It appears to be mainly related to the increase in the strength of the matrix at low temperatures (caused by the freezing of water in the capillary pores), which increases the energy required for fiber pull-out, the main mechanism of energy absorption. The increase in toughness was observed both for normal concretes (with a water/binder ratios of 0.45) and high performance concretes (with a water/binder ratio of 0.30), and for two very different type of fibers at two dosages (40 and 60 kg/m^3). The results further show that, in this type of test, the influence of the fiber geometry is not extremely large, either at normal or at low temperatures.

ACKNOWLEDGEMENTS

The authors are grateful to Ciment St-Laurent and to the Natural Sciences and Engineering Research Council of Canada for their financial support for this project. Special thanks are also due to Professor N. Banthia, of the University of British Columbia, and to Denys Allard, from Ciment St-Laurent, for their advice throughout the project.

REFERENCES

1. Fiber Reinforced Concrete—Modern Developments, Second University-Industry Workshop on Fiber Reinforced Concrete, Toronto, March 1995, ed. N. Banthia & S. Mindess.
2. Dorlot, J.-M., Bailon, J.-P. & Masounave, J., *Des Matériaux*, Éditions de l'École Polytechnique de Montréal, 1986.
3. Wittmann, F. H., *Influence of Time on Crack Formation and Failure of Concrete, Applications of Fracture Mechanics to Cementitious Composites*, ed. S. P. Shah. NATO-ARW, Northwestern University, 1984, pp. 443–464.
4. Miura, T., The properties of concrete at very low temperatures. *Materials Struct./Matériaux et Constructions*, **22** (1989) 243–254.
5. Stavena, P., Sakai, K., Horigushi, T. & Banthia, N., Flexural behavior of steel fiber reinforced concrete

under low temperatures. *Proc. Japan. Concr. Inst.*, 1992, pp. 1.6–6.6.
6. Banthia, N. & Mani, M., Toughness indices of steel fiber reinforced concrete at sub-zero temperatures. *Cement Concr. Res.*, **23** (1993) 863–873.
7. Banthia, N. & Trottier, J.-F., Toughness of concrete reinforced with deformed steel fibers. *ACI Materials J.*, **92**(2) (1995) 146–154.
8. Morgan, D. R., Mindess, S. & Chen, L., Testing and specifying toughness for fiber reinforced and shotcrete. *Fiber Reinforced Concrete — Modern Developments, Second University-Industry Workshop on Fiber Reinforced Concrete, Toronto, March 1995*, ed. N. Banthia & S. Mindess, 1995, pp. 29–50.